

Femtosecond nonlinear optics of the atmosphere

V.P. Kandidov, O.G. Kosareva, E.I. Mozhaev, and M.P. Tamarov

M.V. Lomonosov Moscow State University, Moscow

Received April 20, 2000

Experimental and theoretical investigations into the propagation of high-power laser pulses in the atmosphere are reviewed. The process of filamentation of a high-power femtosecond laser pulse is considered as evolution of the static and dynamic instability of the light field under conditions of strong nonlinearity. The process of initiation of a filament bunch in a TW-power pulse of a femtosecond lidar has been numerically studied, and the results of this study are presented. The influence of the linear dispersion of the group velocity in air on the spatiotemporal intensity distribution of a high-power femtosecond laser pulse is analyzed.

Recent advances in femtosecond laser technology allow new problems to be formulated in the atmospheric optics studies. High energy density and a wide spectral band typical of a high-power laser pulse in air essentially extend the information content of laser sensing and spectroscopic study of the atmosphere and offer new possibilities of remotely determining chemical composition of atmospheric admixtures by using the methods of fluorescent and emission spectral analysis.

The character of nonlinear-optics interaction of laser pulses with the air changes qualitatively with the transition from the milli- and microsecond pulse duration to the femto- and picosecond one.¹ Instead of scattering of light energy because of thermal blooming, optical breakdown, and other nonlinear effects having low thresholds for long pulses, concentration of laser energy and generation of directed white light occur. The problems associated with the study of peculiarities in propagation of high-power laser radiation of femto- and picosecond duration under atmospheric conditions form a new field, which can be called femtosecond nonlinear optics of the atmosphere.

In this paper we review experimental and theoretical investigation into the phenomenon of filamentation arising when high-power laser radiation propagates in the atmosphere. The results of stochastic simulation of the process of atmospheric formation of a filament beam in a TW femtosecond laser pulse are presented. The influence of the material dispersion of gaseous components of air on the character of nonlinear-optics distortions of the laser pulse is discussed.

1. Experimental investigations

Nonlinear atmospheric optics of femtosecond radiation dates back to the mid-90's, when the phenomenon of filamentation at propagation of high-power femtosecond laser pulses in air was discovered in research laboratories of the USA, France, and Canada.^{2,3,4}

In these experiments, the radiation from a Ti:Sapphire laser at 775–800 nm with the pulse duration of 150–230 fs and peak power of 5–50 GW was used, and filaments from tens to hundreds meters long were observed. Filaments are remarkable because more than 10% of pulse energy remains localized in a narrow near-axis region 100 μm in diameter all over the filament length.

The phenomenon of filamentation is accompanied by a conic emission – emission of visible broadband radiation which propagates in the forward direction within a narrow cone enveloping the filament.^{3,5} Now conic emission is considered as a source of pulsed radiation for laser sensing and monitoring of the atmosphere. First encouraging experiments with femtosecond lidars of TW-power were conducted in Germany.^{6,7}

The radiation of a “T⁴-laser” (tabletop terawatt Ti:Sapphire laser) at the wavelength of 790 nm with the duration of 100 fs (at halfmaximum), the maximum pulse energy of 200 mJ, and the pulse repetition rate of 10 Hz was emitted along a vertical path. Filamentation produced an extended channel of laser plasma, which formed a sensing pulse directed in the forward direction with the spectrum covering a band from 500 to 750 nm. The receiving system with an aperture diameter of 40 cm and a $f/3$ telescope had a multichannel recording system sensitive in the spectral band from 350 to 850 nm. In these experiments, the backscattering signal from an altitude of 12 km was detected, and the absorption spectra of oxygen in the band of 758–772 nm and water vapor in the band of 826–836 nm at an altitude of 600–800 m were measured.

The phenomenon of filamentation occurs if two conditions hold: the ultrashort duration of a pulse and high power density. According to experimental data, one filament is formed if the peak power per pulse six to eight times exceeds the critical power of self-focusing for air. It should be noted that the longitudinal size of a subpicosecond pulse is several tens microns, and propagation of such a pulse is, in fact, a flight of a

light bullet – blob of the light field with the power density about 10^{11} – 10^{13} W/cm². The strong nonlinear-optics interaction of the light bullet with the gaseous constituents of the atmosphere and the plasma induced by it cause redistribution of intensity and provokes spatiotemporal instability in the micron-size bullet. Because of the Kerr self-focusing, the intensity peak of 10^{13} – 10^{14} W/cm² is formed, which is followed by a dynamic ring structure produced due to the aberration defocusing in the laser plasma.⁸

Contraction of the light field to a nonlinear focal region leads to the spatiotemporal localization of the radiation energy. A thin trace drawn in air by the nonlinear focus causing glow of aerosol particles in the strong light field forms a visible filament. Rings around the filament alternatively contract to its axis and move apart again in the process of propagation. As a result, the amount of energy passing through a diaphragm changes nonmonotonically along the filament. This phenomenon is called the refocusing effect and it was studied in detail in Refs. 4 and 9.

In recent years some experiments have been conducted on propagation of high-power femtosecond laser pulses in the air and liquids. In connection with the discussions on the theoretical model of propagation, in Ref. 10 filamentation of a focused beam was obtained and a 70-cm long filament was recorded behind the geometrical focus of a lens with the focal length of 2 m. To study the coherence of the radiation re-emitted into a cone, filamentation in water, methanol, and CCl₄ was studied in Refs. 9 and 11. As was shown based on measurement data obtained with a Michelson interferometer, the conic radiation in the band of 500–800 nm has the same coherence length as the initial laser pulse at 800 nm wavelength.

Vast experimental material has been obtained in Ref. 12 for high-power femto- and subpicosecond laser radiation at the wavelengths of 1053 and 795 nm with 500 and 60-fs long pulses having the peak power of 20–40 and 150–300 GW, respectively. For the 60-fs long pulses the filament length exceeded 200 m. For the pulses of subpicosecond duration a filament was observed at a distance from 4 to 50 m. In this case, its energy dropped down from 9 to 2 mJ at the initial pulse energy of 15 mJ. At the peak power of 30 GW, which seven to eight times exceeded the critical power of self-focusing in air at the wavelength of 1053 nm, formation of three to four filaments at a short distance was observed. It was noticed that not all intensity perturbations arising in the beam cross section at the initial stage of propagation led to formation of filaments. By the method of longitudinal interferometry, it was determined in Ref. 12 that the initial density of electrons in the formed laser plasma several times exceeded the level of 10^{16} cm⁻³.

The random nature of filamentation mentioned in Ref. 12 was earlier noticed in Ref. 4, in which a random shift of a filament in the recording plane was observed. To decrease these wandering, the trajectory of a pulse was enclosed within a “channel” which was

fenced off by cardboard boxes. In experiments with a femtosecond laser,^{6,7} whose peak pulse power several hundreds times exceeded the critical power of self-focusing in air, a beam of filaments was formed. Since the appearance of filaments is random under conditions of natural atmospheric turbulence, a collecting lens with the focal length of 30 m was used for regularizing the formation of many filaments. In the vicinity of caustic of this lens an extended plasma channel occurred that emitted a directed white light. Analysis of the available experimental data reveals a significant influence of atmospheric turbulence and, possibly, spatial coherence of the beam emitted by the laser, on the process of initiation and formation of filaments at propagation of a high-power femtosecond pulse under real atmospheric conditions.

2. Theoretical models

Theoretical investigations into the nonlinear atmospheric optics of femtosecond radiation are based on the approximation of the method of slowly varying amplitudes, which remains valid for pulses with the duration up to three periods of optical oscillations.¹³ The nonlinear-optics interaction of femtosecond radiation with air includes the cubic, in terms of the field, response from the gas molecules. This response is determined by the increment of the refractive index $\Delta n_k(I)$, response $\Delta n_p(I)$ of the laser plasma arising in the strong light field, and nonlinear absorption with the coefficient $\alpha_z(I)$. The nonlinearities connected with the induced changes in the air temperature and density are ignored, because in the case with the femtosecond pulses the process of thermalization of the absorbed light energy proves to be too slow and these effects, which have the lowest energy threshold for long pulses, have no time to manifest themselves. Fluctuations of the refractive index in the turbulent atmosphere are described by a random stationary field $\tilde{n}(r)$. According to the commonly accepted ideas, we can write the following equation for the complex amplitude E of the electric field:

$$2ik \left(\frac{\partial}{\partial z} + \frac{1}{v_g} \frac{\partial}{\partial t} \right) E = \Delta_{\perp} E - k \frac{\partial^2 k}{\partial \omega^2} \frac{\partial^2 E}{\partial t^2} + 2k^2 \Delta n_k E + 2k^2 \Delta n_p E + 2k^2 \tilde{n} E - ik\alpha_z E. \quad (1)$$

The time of establishment of the response from molecules is comparable with the pulse duration. Therefore the dependence of the increment Δn_k on the intensity I is determined by the equation

$$\Delta n_k(I) = (1 - g) n_2 I + gn_2 \int H(t - t') I(t') dt'. \quad (2)$$

Here the first term corresponds to the instantaneous response caused by the electron Kerr effect in air,¹⁴ the second term describes the time lagged part of the response with the pulsed transient

function $H(t - t')$. In the case of the orientation Kerr effect,¹⁴ the function $H(t - t')$ describes the relaxation process with the time of establishment about 10^{-13} s.

In Ref. 15 the time lagged response in air was related to Raman scattering involving rotational transitions. In this case, the transient function $H(t - t')$ corresponds to decaying oscillations. In Eq. (2) the weighting factor $g < 1$. The coefficient n_2 is equal to the value determined for the stationary Kerr nonlinearity.

The increment of the refractive index Δn_p caused by the plasma depends on the concentration of electrons N_e :

$$\Delta n_p = -2\pi e^2 N_e / (\omega^2 m). \quad (3)$$

Laser plasma arises because of the multiphoton tunnel processes of photoionization as the intensity of the light field increases up to 10^{13} – 10^{14} W/cm² in the process of Kerr self-focusing. For femtosecond laser plasma in air, we can neglect recombination of ions, whose time is about 10^{-11} s, collisional ionization, electron drift, and effects connected with the waves of the electron density.¹⁶ Then, in the single ionization approximation, which is valid at relatively low intensity ($I < 10^{14}$ W/cm²), we can write the following kinetic equation describing the increase of the electron concentration with time:

$$\partial N_e / \partial t = R(I) (N_0 - N_e), \quad (4)$$

where $R(I)$ is the rate of photoionization of oxygen molecules, which is set in accordance with the accepted theoretical model (see, for instance, Refs. 17, 18, and 19). The contribution of other components of air to the formation of plasma can be neglected, since the ionization potential of nitrogen is higher than that of oxygen, and the concentration of other components is low. The absorption coefficient $\alpha_\Sigma(I)$ caused by energy loss at photoionization is

$$\alpha_\Sigma = I^{-1} l \hbar \omega (\partial N_e / \partial t), \quad (5)$$

where l is the number of photons involved in the process of ionization ($l = 7 - 8$).

The initial distribution of the field $E(x, y, z = 0, t)$ in the pulse is assumed to be Gaussian over space and time, what agrees with the experimental data:

$$E(x, y, z = 0, t) = E_0 \exp\left(-\frac{x^2 + y^2}{2a^2} - \frac{t^2}{2\tau_0^2}\right). \quad (6)$$

The formulated problem (1)–(6) on propagation of a high-power laser pulse in the turbulent atmosphere can be characterized as stochastic, nonlinear, dynamic, and multidimensional. Analysis of this very complicated problem in its complete formulation is now impossible. Therefore, investigators now usually restrict themselves to the study of filamentation in the absence of fluctuation of the refractive index in air. In this case, the problem is axisymmetric, what significantly

simplifies its numerical and analytical consideration. In Refs. 1, 4, and 8, physical interpretation of filamentation is given based on numerical analysis with the use of the model of moving focus supplemented with the nonstationary nonlinear-optics process of radiation interaction with the self-induced laser plasma. This model has allowed the effect of refocusing and appearance of conic emission observed in the experiments to be explained.

In the papers by French scientists,^{3,20} similar results of numerical solution are relied on to explain the phenomenon of filamentation from the viewpoint of “self-channeling” at mutual compensation of stationary self-focusing and aberration defocusing in the nonstationary laser plasma. The nonmonotonic change of the intensity at the filament axis found from numerical analysis of the set of equations (1)–(6) with $\tilde{n} = 0$ is defined as the process of spatiotemporal replenishment of the light field.²¹ The variational method similar to that developed in Refs. 22 and 23 was applied in Ref. 24 to the set of equations (1)–(6) in the stationary formulation. The functional has been written for this set of equations, which was minimized by the Galerkin method,²⁵ according to which the variation of the conservative part of the functional is equated to the energy loss of the light field. The basis functions, within which class of the light field distribution over the beam cross section is sought, are chosen in the form of a Gaussian profile. In Ref. 24 the equations for the width of the Gaussian profile filament and the curvature of the wave front were derived and solved.

3. Spatiotemporal instability. Influence of the atmospheric turbulence

From the general point of view, the phenomenon of filamentation, in which a complex dynamic structure of intensity distribution in the beam cross section is formed, is a result of light field instability evolving under conditions of optical nonlinearity. Following the definitions given in Ref. 26, the statistical instability of the light field, at which the intensity peak increases rapidly, at Kerr self-focusing gives way to the dynamic instability caused by nonstationary defocusing in the self-induced plasma. The dynamic instability manifests itself as a system of rings varying in space and time.

At formation of one filament in a regular medium, the instability of the light field originates at the beam axis, where the intensity is maximum. However, under real conditions the point of filament formation in the beam cross section is mostly determined by turbulent fluctuations of the refractive index. The origin of a filament is caused by the Kerr self-focusing in a randomly inhomogeneous medium and does not depend on the plasma that is being initiated later on. This is described by Eq. (1) with $\Delta n_p = 0$, $\alpha_\Sigma = 0$. The statistical instability of the field is also independent of the dispersion of the group velocity.

In Ref. 27 the origin and the initial stage of formation of a filament in the turbulent atmosphere were simulated numerically at this formulation of the problem and at $\tilde{n} \neq 0$. The fluctuations of the refractive index in air were simulated by the chain of phase screens generated by the method of subharmonics²⁸ allowing a wide spatial spectrum of atmospheric turbulence to be reproduced. Intensity perturbations caused by fluctuations of the phase of the light field in the atmosphere play the part of a seed for the statistical instability to occur, whose evolution is most probable near the beam axis where the light intensity is the highest. However, at $P \leq (6-10)P_{\text{crit}}$ only one of the intensity peaks increases with distance thus forming a filament. As a result, a filament originates at a random point in space.

By the method of statistical tests it was determined that the distance from the exit aperture of the laser to the plane of filament formation decreases, on average, under turbulent conditions. This is explained by the fact that random focusing of light field in the atmosphere favors more rapid evolution of the nonlinear focus because of statistical instability of the positive intensity fluctuations. As analysis shows, the variance of cross shifts of a filament increases with distance and reaches several millimeters at a distance of several tens meters.

At a small distance from the exit aperture of the laser, the shift of filament markedly exceeds the shift of the intensity centroid of a low-power beam under the same conditions of propagation (Fig. 1). From that it follows that deviation of the point of nonlinear focus origination due to smallest-scale fluctuations in the atmosphere makes a decisive contribution to the transverse wandering of the filament beginning. The farthest part of the filament is at a long distance from the laser and its wandering is mostly caused by the deflections of its propagation direction due to atmospheric inhomogeneities exceeding the cross size of the laser beam.

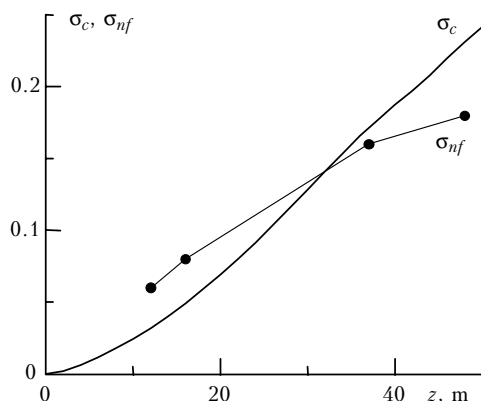


Fig. 1. The RMS shift of a filament σ_{nf} (curve with dots) and the RMS deviation from the centroid of low-intensity beam σ_c (solid curve) vs. the path length z in the atmosphere with the parameters $C_n^2 = 5 \cdot 10^{-15} \text{ cm}^{-2/3}$, $l_0 = 1 \text{ mm}$, $L_0 = 1 \text{ m}$. The peak power of the pulse forming the filament is $P_0 = 36 \cdot 10^9 \text{ W}$, the beam radius is $a = 3.5 \text{ mm}$.

Propagation of radiation with the peak power $P = 2.2 \cdot 10^{12} \text{ W}$ and the initial radius of the laser beam $a = 3 \text{ cm}$ in the atmosphere was considered in Ref. 6 for stochastic simulation of formation of a bunch of filaments initiated by a femtosecond laser pulse. The beam was assumed to be of the Gaussian profile and collimated, in contrast to Ref. 6. It is important that refractive index fluctuations of all scales are significant in the formation and wandering of filaments. The character of influence of the atmospheric inhomogeneities changes during the formation of filaments. Thus, millimeter inhomogeneities are small-scale for the initial beam and cause the appearance of nonlinear focuses in its cross section. However, then in the process of formation of the intensity peak having the cross size of several hundreds microns, the same inhomogeneities become large-scale and contribute to the shift of the filament. Therefore, to simulate atmospheric turbulence, the modified von Karman spectrum was used²⁹

$$\Phi_n(\mathbf{r}) = 0.033 C_n^2 (\mathbf{r}^2 + \mathbf{r}_0^2)^{-11/6} \exp\{-\mathbf{r}^2/\mathbf{r}_l^2\}, \quad (7)$$

where $\mathbf{r}_0 = 2\pi/L_0$, $\mathbf{r}_l = 5.92/l_0$. It is natural to take the inner scale l_0 equal to 1 mm.

Since the structure constant C_n^2 and the outer scale of turbulence L_0 were not measured in the experiment, it was assumed that these parameters do not vary with distance. Under conditions of strong turbulence characteristic of the urban environment, where the experiment was conducted, it can be taken to be equal to $C_n^2 = 5 \cdot 10^{-15} \text{ cm}^{-2/3}$, $L_0 = 1 \text{ m}$. For simulation of atmospheric turbulence with the spectrum (7), the chain of statistically independent phase screens set in the step of 1 m one behind other was used. The phase screens were generated by the method of subharmonics with two iterations.²⁸ The interval, in which the nonlinear phase change was calculated, decreased with the increasing intensity in the process of self-focusing. In the numerical experiment, a 1024×1024 square grid with the step $h = 0.4 \text{ mm}$ in the plane XOY was used.

Figure 2 shows the isophots in the beam cross section at different distances from the exit aperture of a lidar. It is seen that the random intensity distribution arises because of the turbulence. The set of most intense peaks in the beam cross section increases rapidly with distance thus forming a bunch of filaments. The distances, at which filaments are formed and the power in them achieves the ionization threshold, are different. For a model medium without fluctuations ($\tilde{n} = 0$) numerical analysis of the problem on formation of a bunch of filaments losses physical sense. The results of such analysis are presented in Ref. 30, in which the spatial instability of the light field originates at nodes of a rectangular computational grid. The regular structure of speckles varying in time was defined in Ref. 30 as optical turbulence.

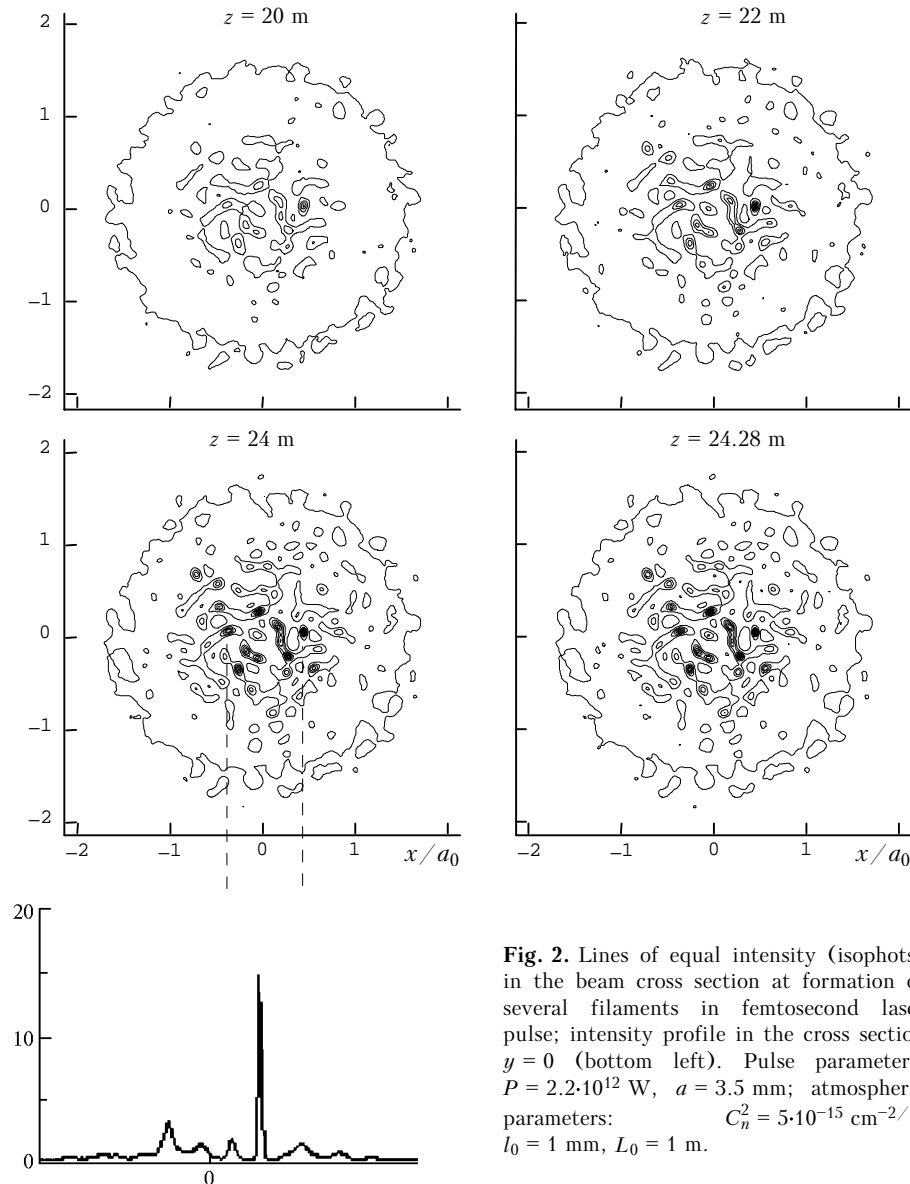


Fig. 2. Lines of equal intensity (isophots) in the beam cross section at formation of several filaments in femtosecond laser pulse; intensity profile in the cross section $y = 0$ (bottom left). Pulse parameters: $P = 2.2 \cdot 10^{12}$ W, $a = 3.5$ mm; atmospheric parameters: $C_n^2 = 5 \cdot 10^{-15} \text{ cm}^{-2/3}$, $l_0 = 1$ mm, $L_0 = 1$ m.

4. Influence of the dispersion of the group velocity on dynamic instability of a light pulse

In evolution of the spatiotemporal instability of the light field in a nonlinear medium, the time lag of its response plays a significant part. Analysis performed in Ref. 31 by the method of perturbations showed that dynamic instability of the light field arises in inertialess nonlinear media as a result of joint manifestation of the dispersion of group velocity, phase self-modulation, and diffraction. In its turn, if there is no linear dispersion in a medium, then spatiotemporal instability can evolve only in the case of a time lagged nonlinear response, i.e., dispersion of nonlinearity.²⁶

For high-power femtosecond pulses in air the dispersion of nonlinearity manifests itself in

nonstationarity of the nonlinear response of the self-induced laser plasma, electrons in which are accumulated during the pulse. The material dispersion of the group velocity in air is low for the initial subpicosecond pulse. It can be estimated by Cauchy equation, which has the following in case of standard atmospheric conditions³²:

$$n(\lambda) = [2726.43 + (12.29 \cdot 10^{-6} \text{ nm}^2) / \lambda^2] \cdot 10^{-7} + 1. \quad (8)$$

With a pulse $2\tau_0 = 276$ fs long at the wavelength $\lambda_0 = 800$ nm, for example, the dispersion length is $L_{\text{disp}} \approx 1200$ m. The allowance for the fine structure of the spectral absorption lines of the gaseous atmospheric components leads to insignificant dispersion distortions of the subpicosecond pulse along a path several kilometers long.³³ This is connected with the fact that a large number of weak narrow spectral lines fall within the spectral band of such a pulse.

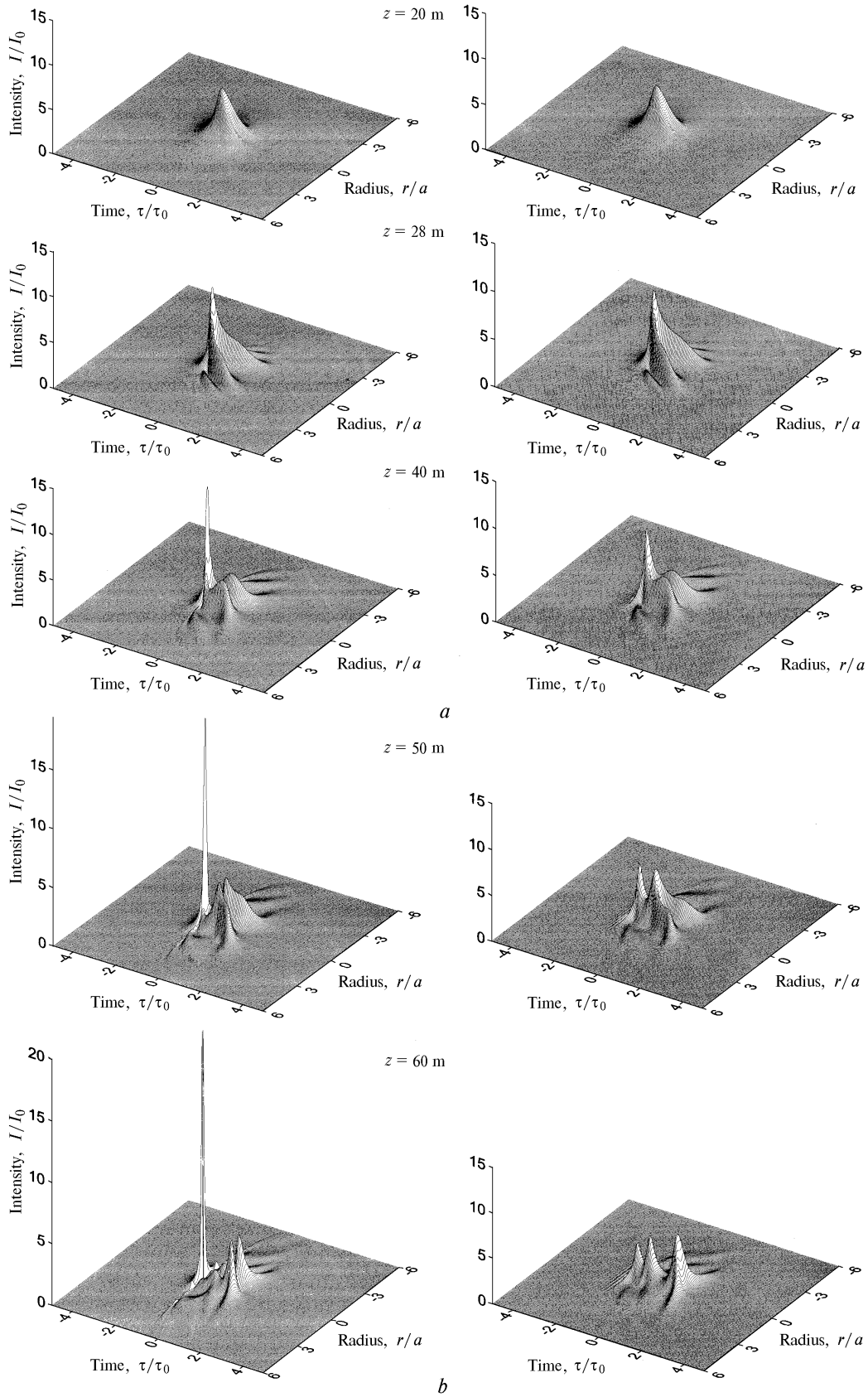


Fig. 3. Spatiotemporal intensity distribution vs. distance at filamentation of laser pulse with peak power $P_0 = 36 \cdot 10^9$ W ($P_0 = 6.3 P_{\text{crit}}$), pulse duration at half-maximum level $\tau_0 = 138$ fs, and normalized beam radius corresponding to $a = 3.5$ mm: with (right-hand panels) and without (the left-hand ones) the account of linear dispersion of group velocity.

It seemingly follows from the above analysis that the influence of linear dispersion of the group velocity on propagation of the subpicosecond laser pulse is negligibly small, since the filament length is about 100 m. However, the pulse sharpens markedly in the process of self-focusing and nonlinear refraction in plasma. The duration of the formed peak shortens down to several tens femtoseconds, and the influence of the dispersion of group velocity becomes significant. This is supported by the results of numerical experiment conducted for the air without fluctuations at $\bar{n} = 0$. The pulse with the peak power $P = 6.3 P_{\text{crit}}$ was considered, where P_{crit} is the critical power of self-focusing. The initial beam radius was $a = 170 \mu\text{m}$, pulse duration at half-maximum level was $\tau_0 = 138 \text{ fs}$, and the peak intensity was $I_0 = 10^{13} \text{ W/cm}^2$.

Figure 3 shows the spatiotemporal distribution of the intensity I in a pulse at different distance z from the exit aperture. Here the running time $\tau = t - z/v_g$ is introduced, which starts ($\tau = 0$) at the center of a pulse. At $z = 20 \text{ m}$, distortions of the pulse are relatively small, and the intensity distribution still remains unimodal. Due to self-focusing, the intensity peak increases several times and shifts insignificantly toward the pulse tail. As the intensity I increases, multiphoton ionization of oxygen molecules occurs. This ionization has a threshold character because of a sharp increase in the ionization rate: $R(I) \sim I^8$. The influence of defocusing in the laser plasma manifests itself in restriction of the intensity growth in the nonlinear focus and in origination of the ring structure at the pulse tail. For the coordinates τ/τ_0 and r/a used in Fig. 3, the ring structure in the pulse tail manifests itself in the fact that the intensity, as a function of radius r , in the cross section $\tau/\tau_0 = \text{const}$ ($\tau/\tau_0 \geq 1$) has minimum at the axis $r = 0$ and two symmetric maxima.

As the distance z increases, dynamic instability evolves in the pulse tail. Several pronounced rings arise in the intensity distribution. At $z = 40, 50 \text{ m}$ they contract to the beam axis and their intensity changes. Such a change of the light field is explained by the effect of refocusing which was observed experimentally.⁴

At the distance $z = 20 \text{ m}$, the linear dispersion of the group velocity has no effect on the pulse propagation, because its temporal scale has not changed significantly. Analyzing the influence of the linear dispersion of the spatiotemporal intensity distribution at $z > 20 \text{ m}$, we can note the following.

First, linear dispersion significantly restricts the intensity growth at Kerr self-focusing. At the leading edge of the pulse, where the power is lower than at the center, Kerr self-focusing occurs at long distances. In this case, in the absence of linear dispersion the sharpness of the formed peak increases rapidly and the time of photoionization in the strong light field shortens. Under these conditions, the concentration of

electrons sufficient for defocusing in plasma is achieved at a higher intensity of the peak. Therefore, its value increases, while the duration decreases. The linear dispersion in air slows down the intensity growth at self-focusing, the time of generation in the peak increases, and defocusing in plasma manifests itself at lower intensity in the peak thus restricting its value.

Second, the dispersion of the group velocity qualitatively changes the pattern of the intensity distribution at the pulse tail. At long distances ($z = 60 \text{ m}$) a set of peaks is formed in place of rings obtained when neglecting linear diffraction. The disintegration of the pulse into peaks is a result of the joint effect of the dispersion of the group velocity and phase self-modulation in a nonlinear medium.³⁴

As analysis shows, the linear dispersion in air significantly influences the frequency-angular spectrum of the pulse. The short-wave part of this spectrum resulting from spatiotemporal self-modulation of the phase of the light field forms the conic emission.⁵

Conclusion

Femtosecond nonlinear optics of the atmosphere is now only in the beginning of its development. It covers a wide variety of both fundamental and applied problems to be solved. These problems include, for example, study of the influence of atmospheric aerosol on filamentation, analysis of coherence of the sensing femtosecond laser pulse, processes of emission and fluorescence of atmospheric constituents under the effect of a femtosecond pulse, problems of optimization of the parameters of laser radiation for the purposes of atmospheric monitoring.

Acknowledgments

This work was partially supported by the Russian Foundation for Basic Research, Grant No. 00-02-17497.

References

1. V.P. Kandidov, O.G. Kosareva, A. Broder, and S.L. Chin, *Atmos. Oceanic Opt.* **10**, No. 12, 966-973 (1997).
2. A. Braun, G. Korn, X. Liu, D. Du, J. Squier, and G. Mourou, *Opt. Lett.* **20**, 73 (1995).
3. E.T.J. Nibbering, P.F. Curley, G. Grillon, B.S. Prade, M.A. Franco, F. Salin, and A. Myszyrowicz, *Opt. Lett.* **21**, 62 (1996).
4. A. Brodeur, O.G. Kosareva, C.Y. Chien, F.A. Ilkov, V.P. Kandidov, and S.L. Chin, *Opt. Lett.* **22**, 304 (1997).
5. O.G. Kosareva, V.P. Kandidov, A. Brodeur, C.Y. Chien, and S.L. Chin, *Opt. Lett.* **22**, 1332 (1997).
6. L. Woste, C. Wedekind, H. Wille, P. Rairoux, B. Stein, S. Nikolov, Chr. Werner, St. Neidermeier, F. Ronneberger, H. Schillinger, and R. Sauerbrey, *Laser and Optoelectronik* **29**, No. 5 (1997).
7. L. Woste, C. Wedekind, H. Wille, P. Rairoux, M. Rogriguez, B. Stein, R. Sauerbrey, H. Schillinger, F. Ronneberger, and St. Neidermeier, in: *Ultrafast Phenomena XI, Proc of the 11th Intern. Conf.*, Garmisch-Partenkirchen, Germany (1998), p. 118.

8. O.G. Kosareva, V.P. Kandidov, A. Brodeur, and S.L. Chin, *Nonlinear Opt. Phys. & Mat.* **6**, 485 (1997).
9. S.L. Chin, A. Brodeur, S. Petit, O.G. Kosareva, and V.P. Kandidov, *Nonlinear Opt. Phys. & Mat.* **8**, No. 1, 121 (1999).
10. H.R. Lange, G. Grillon, J-F. Ripoche, M.A. Franko, B. Lamouroux, B.S. Prade, and A. Mysyrowicz, *Opt. Lett.* **23**, 120 (1998).
11. S.L. Chin, S. Petit, F. Borne, and K. Miyazaki, *Jpn. J. Appl. Phys.* **38**, Part 2, No. 2A, L126 (1999).
12. B.L. Fontaine, F. Vidal, Z. Jiang, C.Y. Chein, D. Comtois, A. Desparois, T.W. Johnston, J-C. Kieffer, H. Pepin, and H.P. Mercure, *Phys. of Plasma* **6**, No. 3, 1815 (1999).
13. S.A. Akhmanov, V.A. Vysloukh, and A.S. Chirkin, *Optics of Femtosecond Laser Pulses* (Nauka, Moscow, 1988), 312 pp.
14. V.V. Zuev, A.A. Zemlyanov, and Yu.D. Kopytin, *Nonlinear Optics of the Atmosphere* (Gidrometeoizdat, Leningrad, 1989), 256 pp.
15. E.T.Y. Nibbering, G. Grillon, M.A. Franko, and A. Mysyrowicz, *J. Opt. Soc. Am.* **B14**, 650 (1997).
16. O.G. Kosareva, "Propagation of high-power subpicosecond laser pulse in gases under conditions of ionization," *Cand. Phys.-Math. Sci. Dissert.*, Moscow State University, Moscow, (1995), 138 pp.
17. A. Szoke, *Atomic and Molecular Processes with Short Intense Laser Pulses*, ed. by A.D. Bandrauk (Plenum, New York, 1987), 207 pp.
18. M.V. Ammosov, N.B. Delone, and V.P. Krainov, *Zh. Eksp. Teor. Phys.* **91**, 2008 (1986).
19. A.M. Perelomov, M.V. Popov, and M.V. Terent'ev, *Zh. Eksp. Teor. Phys.* **50**, 1393 (1966).
20. A. Chiron, B. Lamouroux, R. Lange, J-F. Ripoche, M. Franco, B. Prade, G. Bonnaud, G. Raizuelo, and A. Mysyrowicz, *Eur. Phys. J.* **D6**, 383 (1999).
21. M. Mlejnek, E.M. Wright, and J.V. Moloney, *Opt. Lett.* **23**, 382 (1998).
22. V.V. Vorob'ev, *Thermal Blooming of Laser Radiation in the Atmosphere* (Nauka, Moscow, 1987), 220 pp.
23. V.P. Kandidov, S.S. Chesnokov, and V.A. Vysloukh, *Method of Finite Elements in Problems of Dynamics* (Moscow State University Publishing House, Moscow, 1980), 165 pp.
24. N. Akozbek, C.M. Bowden, and S.L. Chin, *Phys. Rev.* **E** (2000).
25. S.G. Mikhlin, *Variational Methods in Mathematical Physics* (Nauka, Moscow, 1970), 512 pp.
26. V.P. Kandidov, O.G. Kosareva, and S.A. Shlenov, *Kvant. Elektron.* **24**, No. 5, 453 (1997).
27. V.P. Kandidov, O.G. Kosareva, M.P. Tamarov, A. Brode, and S. Chin, *Kvant. Elektron.* **29**, No. 1, 73 (1999).
28. V.P. Kandidov, M.P. Tamarov, and S.A. Shlenov, *Atmos. Oceanic Opt.* **11**, No. 1, 23-29 (1998).
29. S.M. Rytov, Yu.A. Kravtsov, and V.I. Tatarskii, *Introduction into Statistical Radiophysics* (Nauka, Moscow, 1978), Part 2, 463 pp.
30. M. Mlejnek, M. Kolesic, J.V. Moloney, and E.M. Wright, *Phys. Rev. Lett.* **83**, No. 15, 2983 (1999).
31. L.W. Liou et al., *Phys. Rev.* **A 46**, 4202 (1992).
32. *Handbook of Chemistry and Physics* (CRC Press, 1984-1985).
33. V.P. Kandidov and M.P. Tamarov, *Atmos. Oceanic Opt.* **9**, No. 5, 400-404 (1996).
34. P. Chernev and V. Petrov, *Opt. Lett.* **17**, No. 3, 172 (1992).